Does Hydrogen Bonding Matter in Crystal Engineering? Crystal Structures of Salts of Isomeric Ions

Alessandro Angeloni, Paul C. Crawford, A. Guy Orpen,* Thomas J. Podesta, and Benjamin J. Shore[a]

Abstract: The preparation and structure determinations of the crystalline salts [3,3′-H_2bipy][$PtCl_4$] (**2**), [2,2′-H_2bipy][$PtCl_4$] (**3**) and [1,4′-Hbipy][$PtCl_4$] (**4**) and [3,3′-H_2bipy][$SbCl_5$] (**6**) and [1,4′-Hbipy][$SbCl_5$] (**8**) are reported. In addition a redetermination of the structure of the metastable salt [4,4′-H_2bipy][$SbCl_5$] (**5b**) in the corrected space group *Pbcm* is described. These structures are compared to those of the known salt [4,4′-H_2bipy][$PtCl_4$] (**1**), the stable triclinic form of [4,4′-H_2bipy][$SbCl_5$] (**5a**) and [2,2′-H_2bipy][$SbCl_5$] (**7**). In the case of the salts of the rigid $[PtCl_4]^{2-}$ ion, structures **2**, **3** and **4** are essentially isostructural despite the differing hydrogen-bonding capability of the cations. Similarly, among the salts of $[SbCl_5]^{2-}$ ions, structures **7** and **8** are essentially isostructural. Structure **6** differs from these in having a differing pattern of aggregation of the $[SbCl_5]^{2-}$ ions to form polymeric rather than tetrameric units. It is evident that local hydrogen-bonding interactions, although significant, are not the only or even the decisive influence on the crystal structures formed by these salts. These observations are not in good accord with the heuristic "sticky tecton" or supramolecular synthon models for synthetic crystallography or crystal engineering.

Keywords: crystal engineering · electrostatic interactions · hydrogen bonds · organic–inorganic hybrid composites · supramolecular chemistry

Introduction

One of the principal challenges of modern chemistry is that of the crystal engineering of new crystal structures. The ambition of this branch of crystal engineering—which we might better term "synthetic crystallography"—is to design and prepare (grow) novel crystal structures based on molecular building blocks or tectons.[1–3] This is a considerable challenge given the immense difficulties of predicting, ab initio, a crystal structure from knowledge of its molecular components. A widely used approach is to exploit the principles of supramolecular chemistry to achieve desired modes of aggregation through planned "stickiness" of the tectons.[1] Specific intermolecular interactions, termed supramolecular synthons by Desiraju,[4] are used, often based on the hydrogen-bonding ability of the tectons. We and others have employed this strategy to create novel structures based on metal complex anions that accept hydrogen bonds and organic cations with hydrogen-bond-donor capability.[5–9] Similar strategies have been applied to other systems based on salts of carboxylate, sulphonate or diketoenolate anions.[10] In this work the underlying assumption is that the key, structure-determining, features of these structures are the supramolecular synthons (e.g., the NH···Cl_2M hydrogen bond unit **A**), that is to say that the paradigm posited by Desiraju holds.[4] It is clear that this model for crystal structure synthesis is heuristic and that successful synthons must in reality compete with or complement a range of other factors, both thermodynamic and kinetic, in providing access to desired crystal structures. In this paper we address that competition or complementarity through an experimental study.

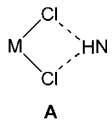

A

In the salt crystal structures that we and others have studied[5–10] it is clear that there are a number of important contributions to the stability of the structures formed, in addition to the hydrogen bonding synthon(s) they show. In particular the complementarity of the shapes of the ions and the electrostatic interactions between those ions must play a significant role in determining the crystal structure. Indeed one might argue that, given the shapes of the complex ionic tectons used in this work ($[MCl_4]^{2-}$ and $[4,4'\text{-}H_2bipy]^{2+}$, for example) and the relatively high charges they carry, that the

[a] Dr. A. Angeloni, P. C. Crawford, Prof. A. G. Orpen, Dr. T. J. Podesta, B. J. Shore
School of Chemistry, University of Bristol
Cantock's Close, Bristol BS8 1TS (UK)
Fax: (+44) 117-929-0376
E-mail: guy.orpen@bristol.ac.uk

Supporting information for this article is available on the WWW under http://www.chemeurj.org/ or from the author. Tables of hydrogen-bonding geometry in structures **1**–**8**.

 DOI: 10.1002/chem.200400165

combination of shape and electrostatic factors might conceivably outweigh the local and directional hydrogen-bonding interactions that we have *assumed* to be critical. In this paper we report an experimental study designed to test the hypothesis that hydrogen bonding matters in this class of crystal structure and more generally in synthetic crystallography. In short we seek to test the Desiraju–Wuest paradigm in this class of structures.

We have addressed the problem by preparation and analysis of a series of crystal structures of the $[PtCl_4]^{2-}$ and $[SbCl_5]^{2-}$ dianions with the isomeric organic dications [4,4′-H_2bipy]$^{2+}$ (**B**), [3,3′-H_2bipy]$^{2+}$ (**C**), [2,2′-H_2bipy]$^{2+}$ (**D**) and [1,4′-Hbipy]$^{2+}$ (**E**). The cations are not only isomeric, but

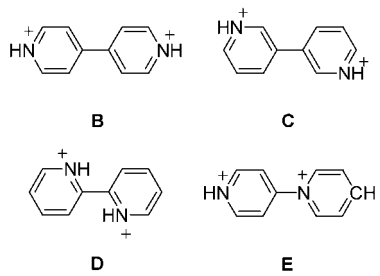

B C D E

might be termed isosteric in that they have to a first approximation very similar volumes and shapes. The dications **B**–**E** are relatively rigid, but have one degree of (partial) conformational freedom about the central C–C (or C–N) bond with both planar and twisted forms of bipyridines and their protonated forms being well known (see reference [11] for a discussion of the energetics of analogous biphenyl systems in gas and solid phases). The anions are of different sorts. Thus $[PtCl_4]^{2-}$ (**F**) is relatively rigid and always close to D_{4h} symmetry,[12] while the $[SbCl_5]^{2-}$ ion (**G**) is much more variable in geometry and is usually self-associated through secondary Sb···Cl interactions forming dimers (**H**), tetramers (**I**) or polymers such as **J**.[13] Valdés-Martínez et al. have reported a related study in which they studied the structures of salts of non-isomeric cations without strong hydrogen-bond-donor capability with anions based on copper and zinc.[14]

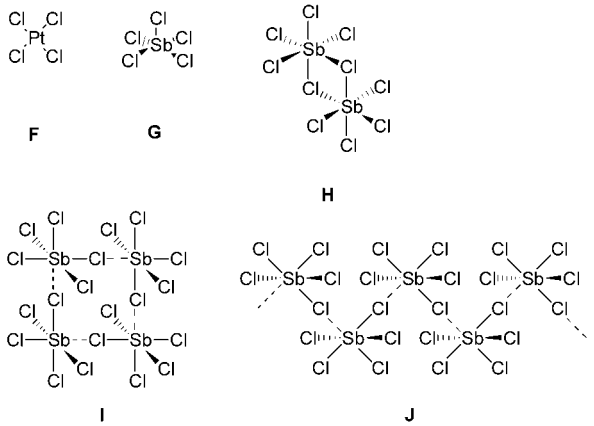

Results

The structure of [4,4′-H_2bipy][$PtCl_4$] (**1**) is known.[5] Samples of [3,3′-H_2bipy][$PtCl_4$] (**2**), [2,2′-H_2bipy][$PtCl_4$] (**3**) and [1,4′-Hbipy][$PtCl_4$] (**4**) were prepared by treatment of salts of $[PtCl_4]^{2-}$ with the appropriately protonated bipyridines (or the chloride salt of the pyridylpyridinium cation in the case of **4**). The salt [4,4′-H_2bipy][$SbCl_5$] is known to have two crystalline forms,[15] one stable and triclinic (**5a**) and the other metastable and orthorhombic (**5b**). We have redetermined the latter structure and show below that the true space group is *Pbcm* and not $Pbc2_1$ as previously reported.[15] In addition the salt [2,2′-H_2bipy][$SbCl_5$] (**7**) is also known.[16] The salts [3,3′-H_2bipy][$SbCl_5$] (**6**) and [1,4′-Hbipy][$SbCl_5$] (**8**) were prepared by treatment of $SbCl_3$ in dilute aqueous HCl with 3,3′-bipyridine to afford **6**, and with the chloride salt of *N*-4′-pyridylpyridinium to give **8**. Single-crystal X-ray diffraction studies of compounds **2**, **3**, **4**, **5b**, **6**, **7** and **8** were carried out in order to establish their structures and provide the information required to assess the effect of the location of the cationic nitrogen centres on these structures. In addition, powder X-ray diffraction studies were carried out on compounds **2**, **3**, **4**, **6**, **7** and **8** in order to confirm that the bulk phase corresponded to that observed in the single-crystal studies. In all cases it was so confirmed.

Platinum salts: The crystallographic details for the structures **1**–**4** are listed in Table 1, and the geometry of their N–H···Cl–Pt hydrogen bonds and the inter-ring torsion angle values are given in Table 2. In structures **1**–**3** both the $[PtCl_4]^{2-}$ ion and the bipyridinium cation lie at a centre of inversion.

The crystal structure of [4,4′-H_2bipy][$PtCl_4$][5,7] (**1**) has a striking planar NH···Cl hydrogen-bonded ribbon motif **K** in

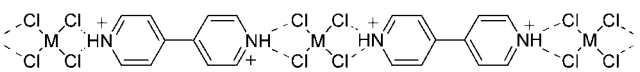

K

which the ions are planar (see Figure 1) and an efficient packing of the ions and their ribbons is achieved (see Figure 2). Good shape fit of anion and cation (see Figure 3) is made around synthon **A**.

Compound **4** contains a mixed NH···Cl_2Pt and CH···Cl_2Pt hydrogen-bond network, containing asymmetric NH···$PtCl_4$···HC moieties, and a polar chain **L**, similar in

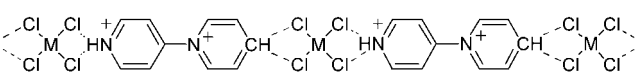

L

form to **K**, results, as shown in Figure 4. The crystal structures of **1** and **4** are both formed from the packing of linear hydrogen bonded chains, as shown in Figure 5. In contrast to the planar chains present in **1**, the chain packing in **4** is nonplanar with the central C–N bond twisted by 39.7° (see Table 2). In addition the chain in **4** is polar with all chains

Table 1. Crystallographic data for platinum compounds **1**–**4**.

	1[5]	**2**	**3**	**4**
formula	$C_{10}H_{10}N_2PtCl_4$	$C_{10}H_{10}N_2PtCl_4$	$C_{10}H_{10}N_2PtCl_4$	$C_{10}H_{10}N_2PtCl_4$
crystal system	monoclinic	monoclinic	monoclinic	monoclinic
M_r	495.09	495.09	495.09	495.09
space group	*I*2/*m*	C_2/c	C_2/c	*Cc*
colour	orange	orange	orange	orange
crystal dimensions [mm]		0.30×0.25×0.25	0.25×0.20×0.20	0.40×0.30×0.30
a [Å]	6.6548(14)	17.153(3)	16.8744(19)	17.333(3)
b [Å]	11.695(2)	7.0207(14)	7.0610(8)	7.090(2)
c [Å]	8.146(3)	12.632(4)	12.6049(14)	12.312(3)
β [°]	91.320(3)	119.214(17)	118.58(2)	119.509(15)
V [Å^3]	633.9(3)	1327.7(5)	1318.8(3)	1316.8(5)
Z	2	4	4	4
μ [mm^{-1}]		11.35	11.43	11.44
ρ_{calcd} [Mg m^{-3}]		2.477	2.494	2.497
$2\theta_{max}$ [°]		54.96	54.95	54.98
reflns collected		4105	4070	4051
independent reflns		1505	1505	2277
R_{int}		0.0336	0.0257	0.0225
R_1 [$I>2\sigma(I)$]		0.0299	0.0287	0.0357
GOF		1.003	1.020	1.073
max/min residual electron density [eÅ^{-3}]		1.45/−1.66	0.605/1.081	1.642/−0.959

Table 2. The NH···Cl hydrogen-bond geometry and central torsion angle values for platinum compounds **1**–**4**.

	N−H···Cl bond length [Å]	NH···Cl bond angle [°]	Inter-ring torsion angle [°]
1	2.40	136.4	0.4
2	2.22	137.1	36.0
	2.43	131.7	
3	2.30	166.4	39.9
4	2.44	152.0	39.7
	2.74	130.3	

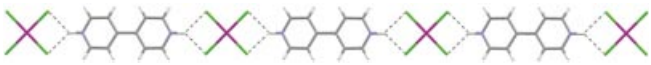

Figure 1. The hydrogen bonded chain in [4,4′-H_2bipy][$PtCl_4$] (**1**).

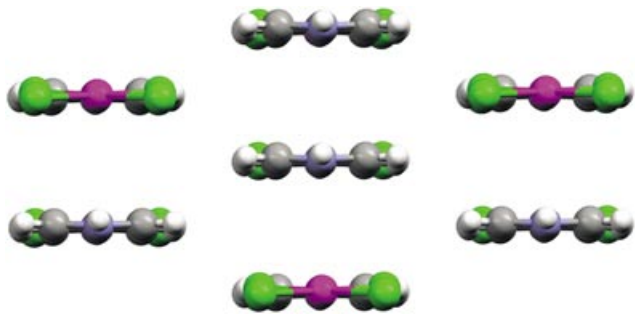

Figure 2. The chain packing in crystalline [4,4′-H_2bipy][$PtCl_4$] (**1**).

parallel to one another. As a consequence the space group of **4** is polar (*Cc*) and the crystal develops macroscopic polarity. That being said, the crystal on which the structure was determined was twinned (twin components in ratio 0.718(15):0.282(15)).

The structures of **2** and **3** are different in respect of the NH···Cl hydrogen bonds present. Compound **2** contains a zig-zag hydrogen-bonded chain (see Figure 6, top) containing the synthon **A** at either end of the 3,3′-bipyridinium ion and the $[PtCl_4]^{2-}$ unit. In compound **3** (see Figure 6, bottom) the 2,2′-bipyridium unit has an *anti* conformation and forms simple (non-bifurcated) NH···Cl–Pt hydrogen bonds at each NH, with only two of the chlorides of each anions involved in NH···Cl bonds. As a result the structure of **3** contains a helical chain of ions linked by NH···Cl contacts (see Figure 6, bottom). Although vestiges remain of the linear chain motif of type **K** (or **L**),

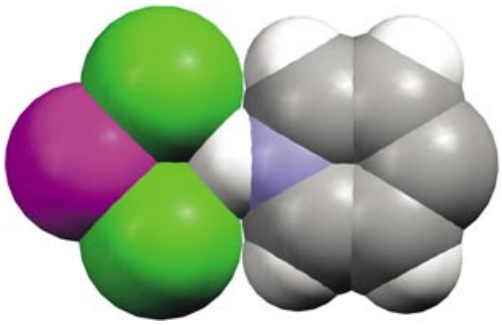

Figure 3. Space-filling diagram of the shape fit in the $PtCl_2$···pyridinium synthon in [4,4′-H_2bipy][$PtCl_4$] (**1**).

Figure 4. The chain motif in [1,4′-Hbipy][$PtCl_4$] (**4**) showing NH···Cl and CH···Cl contacts.

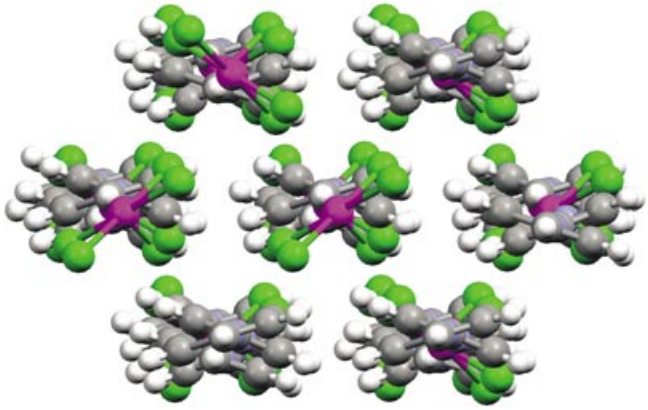

Figure 5. The chain packing in crystalline [1,4′-Hbipy][$PtCl_4$] (**4**).

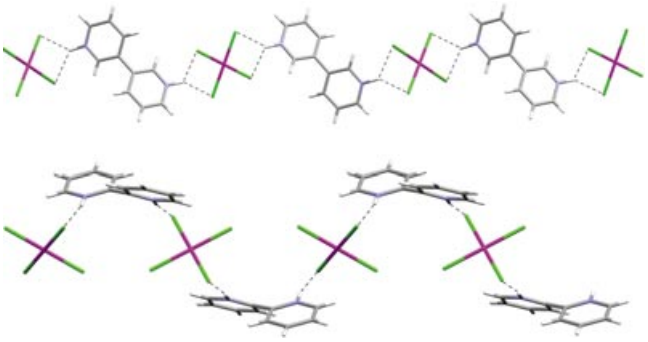

Figure 6. Top: The pattern of NH···Cl hydrogen bonds in [3,3′-H_2bipy][$PtCl_4$] (**2**). Bottom: The pattern of NH···Cl hydrogen bonds in [2,2′-H_2bipy][$PtCl_4$] (**3**).

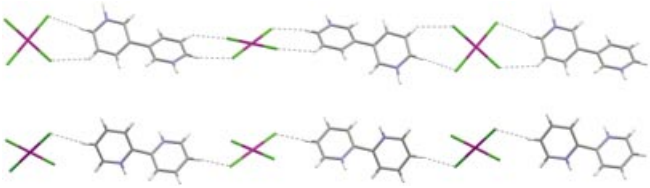

Figure 7. Top: The vestigial chain present in [3,3′-H_2bipy][$PtCl_4$] (**2**) showing CH···Cl contacts <2.95 Å. Bottom: The vestigial chain present in [2,2′-H_2bipy][$PtCl_4$] (**3**) showing CH···Cl contacts <2.95 Å.

but with CH···Cl rather than NH···Cl contacts present in **2** and **3** (see Figures 1 and 7). The packing of these motifs is similar to that seen for **4** (see Figure 2 and Figure 8).

Crystals of **2**, **3** and **4** are essentially isostructural with similar unit cell dimensions and closely related space groups (see Table 1). The molecular packing in all three cases is similar with differences in structure confined to the local distortions required to achieve shorter NH···Cl than CH···Cl contacts (see Supporting Information, Table S1).

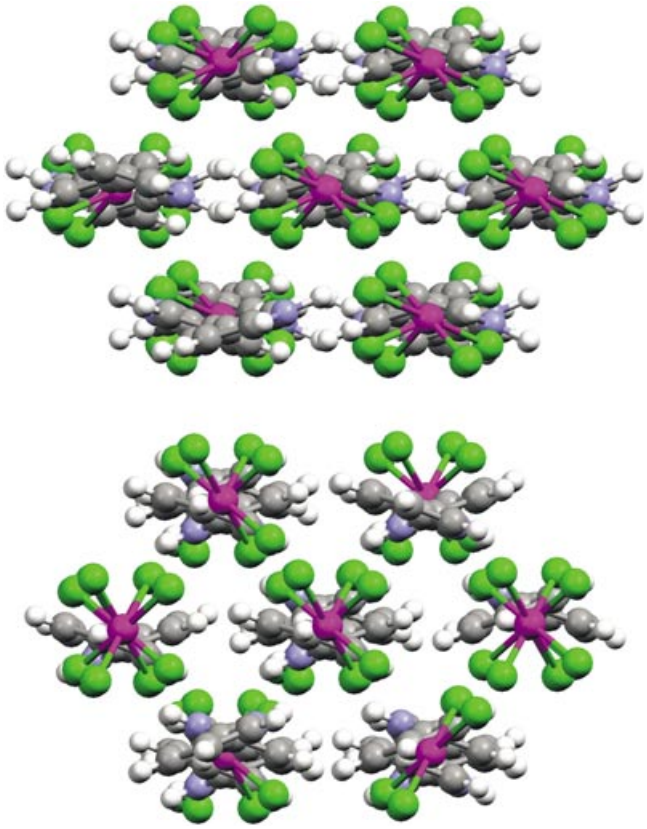

Figure 8. Top: Packing of vestigial chains in [3,3′-H_2bipy][$PtCl_4$] (**2**). Bottom: Packing of vestigial chains in [2,2′-H_2bipy][$PtCl_4$] (**3**).

Antimony salts: The second set of salts is based on $[SbCl_5]^{2-}$ ions in various aggregated forms. The crystallographic details for compounds **5–8** are listed in Table 3 and the geometry of their N–H···Cl–Sb hydrogen bonds and the inter-ring

Table 3. Crystallographic data for compounds **5–8**.

	5a[15]	**5b**	**6**	**7**[16]	**8**
formula	$C_{10}H_{10}N_2SbCl_5$	$C_{10}H_{10}N_2SbCl_5$	$C_{10}H_{10}N_2SbCl_5$	$C_{10}H_{10}N_2SbCl_5$	$C_{10}H_{10}N_2SbCl_5$
M_r	457.20	457.20	457.20	457.20	457.20
crystal system	triclinic	orthorhombic	monoclinic	monoclinic	monoclinic
space group	$P\bar{1}$	*Pbcm*	$P2_1/c$	$P2_1/c$	$P2_1/c$
colour		orange	colourless		yellow
crystal dimensions [mm]		$0.20\times0.20\times0.01$	$0.20\times0.10\times0.01$		$0.40\times0.30\times0.20$
a [Å]	8.431(5)	12.497(2)	14.021(3)	14.109(4)	14.0066(9)
b [Å]	9.586(8)	7.3354(12)	13.836(3)	14.246(11)	14.1428(9)
c [Å]	10.98(1)	16.327(3)	16.641(3)	16.154(10)	16.4614(11)
α [°]	112.45(6)	90	90	90	90
β [°]	101.95(6)	90	109.918(3)	109.36(4)	112.250(1)
γ [°]	97.78(6)	90	90	90	90
V [Å^3]	779.48	1496.7(4)	3035.2(10)	3063.3(4)	3018.1(3)
T [K]	283–303	173(2)	173(2)	283–303	173(2)
Z	2	4	8	8	8
μ [mm^{-1}]		2.718	2.681		2.696
ρ_{calcd} [Mg m^{-3}]		2.029	2.001		2.012
$2\theta_{max}$ [°]		54.98	52.32		55.02
reflns collected		9126	18859		19072
independent reflns		1793	6941		6910
R_{int}		0.0410	0.0655		0.0285
R_1 [$I>2\sigma(I)$]		0.0309	0.0376		0.0303
GOF		0.940	0.899		1.237
max/min residual electron density [eÅ^{-3}]		0.334/−0.734	0.839/−0.835		0.538/−0.605

torsion angle values are given in Table 4. The triclinic, stable polymorph of [4,4′-H_2bipy][$SbCl_5$] (**5**), which has structure **5a**, was shown by Lipka[15] to consist of centrosymmetric anion dimers $[(SbCl_5)_2]^{4-}$ that are linked by hydrogen bonding to $[4,4'\text{-}H_2bipy]^{2+}$ forming a motif of form **K** (see Figure 9, top). In the metastable polymorph **5b** the antimony dianions are polymerised in form **J** (see Figure 9, middle). In both polymorphs the antimony cations form slightly distorted octahedral $SbCl_6$ units through formation of secondary Sb···Cl bonds.[17,18] In **5b** these $SbCl_6$ moieties are cross-linked by hydrogen bonds (see Figure 9, bottom) to the cations into layers of form **M** in a manner previously noted in [4,4′-H_2bipy][MCl_6] (M = Pt, Os).[6] The result of this cross-linking is the formation of a three-dimensional network of secondary (Sb···Cl) and hydrogen bonds (Cl···HN).

Table 4. The NH···Cl hydrogen-bond geometry and central torsion angle values for antimony compounds **5**–**8**.

	N–H···Cl bond length [Å]	NH···Cl bond angle [°]	Inter-ring torsion angle [°]
5a	2.56	136.9	3.0
	2.59	132.9	
	2.58	137.6	
	2.62	130.5	
5b	2.51	139.9	17.2
	2.47	139.0	
6 *syn*	2.29	172.9	11.4
	2.19	169.2	
anti	2.55	148.1	36.0
	2.84	124.2	
	2.27	166.5	
7	2.18	152.9	39.9
	2.21	155.3	41.5
	2.25	164.0	
	2.29	170.8	
8	2.36	170.7	48.0
	2.59	146.5	38.6
	2.87	136.3	

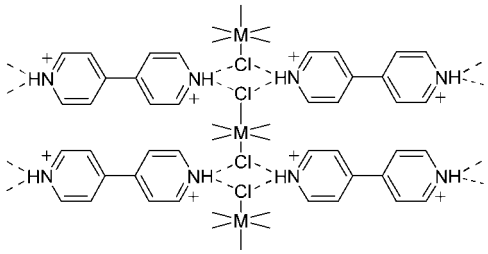

M

The structure of **6** also contains a $[(SbCl_5)_n]^{2n-}$ polymer, albeit of a different form (see Figure 10) to that in **5b**. The chains are cross-linked by NH···Cl hydrogen bonds involving the 3,3′-bipyridium cations and both terminal and bridging chloride ions of the $[(SbCl_5)_n]^{2n-}$ polymer (see Figure 11, top). There are two independent cations of *syn* and *anti* conformations respectively. The packing that results is also shown in Figure 11 (bottom).

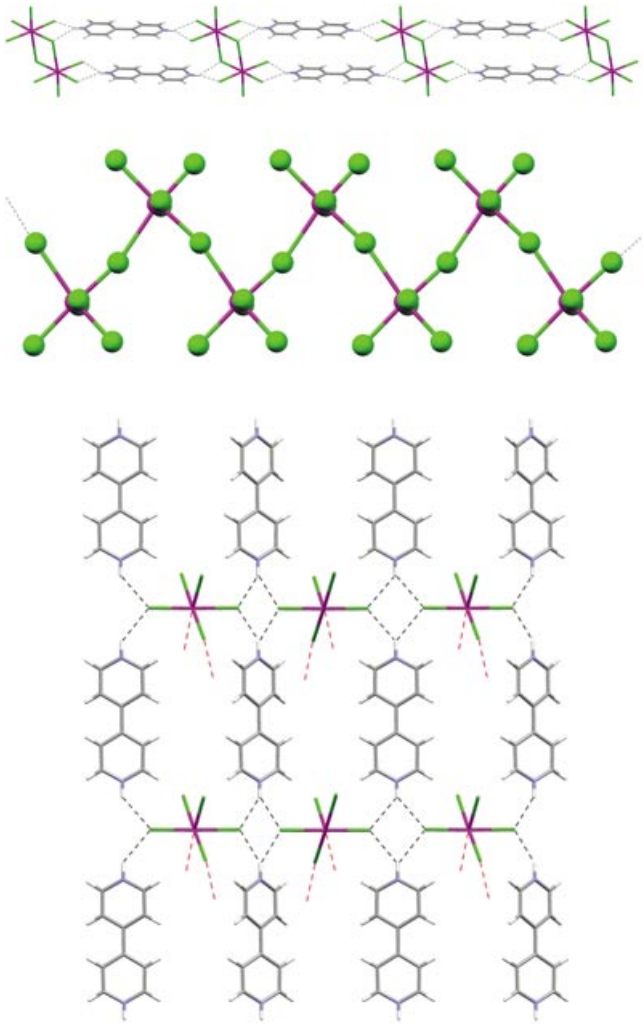

Figure 9. Top: Packing of the double chain of $[(SbCl_5)_2]^{4-}$ dimers and bipyridinium units present in the crystal structure of [4,4′-H_2bipy][$SbCl_5$] (**5a**). Middle: The $[(SbCl_5)_n]^{2n-}$ chain in the metastable crystal structure of [4,4′-H_2bipy][$SbCl_5$] (**5b**). Bottom: Layer formed by hydrogen bonded $[SbCl_5]^{2-}$ and bipyridinium units in the metastable crystal structure of [4,4′-H_2bipy][$SbCl_5$] (**5b**). Contacts between $[SbCl_5]^{2-}$ units in $[(SbCl_5)_n]^{2n-}$ chains are indicated.

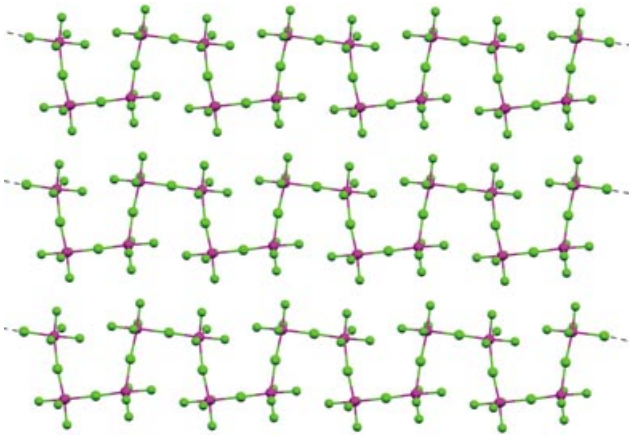

Figure 10. Packing of the $[(SbCl_5)_n]^{2n-}$ chains present in the *ab* plane of the crystal structure of [3,3′-H_2bipy][$SbCl_5$] (**6**).

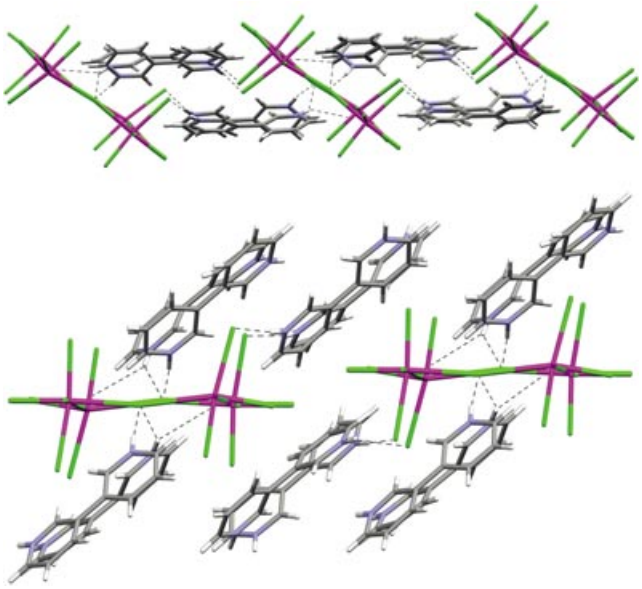

Figure 11. Top: Cross-linking of $[(SbCl_5)_n]^{2n-}$ chains by $[3,3'\text{-bipyH}_2]^{2+}$ cations in the crystal structure of $[3,3'\text{-H}_2\text{bipy}][SbCl_5]$ (**6**) showing the N–H···Cl hydrogen bonds. Bottom: Packing of $[(SbCl_5)_n]^{2n-}$ chains and bipyridinium units present in the crystal structure of $[3,3'\text{-H}_2\text{bipy}][SbCl_5]$ (**6**) viewed parallel to the *ab* plane of the unit cell. The N–H···Cl hydrogen bonds are indicated.

Compounds **7** and **8** are essentially isostructural despite the isomeric nature of their cations. This is reflected in the similarity of the unit cell dimensions and space groups (see Table 3). In both salts the tetrameric anion $[(SbCl_5)_4]^{8-}$ (**I**) is seen and the packing of the ionic tectons is essentially identical. Furthermore they differ only slightly in unit cell dimensions from **6**. The similarity of the packing of the $[(SbCl_5)_n]^{2n-}$ polymer chains in **6** and that of the tetramers in **7** and **8** is notable (see Figures 10 and 12). In **7** each $[(SbCl_5)_4]^{8-}$ unit is involved in eight NH···Cl hydrogen bonds (see Table 4) from eight different dications (see Figure 13, top) while in **8** there are only 4 NH···Cl hydrogen bonds per tetrameric anion (see Figure 13, bottom).

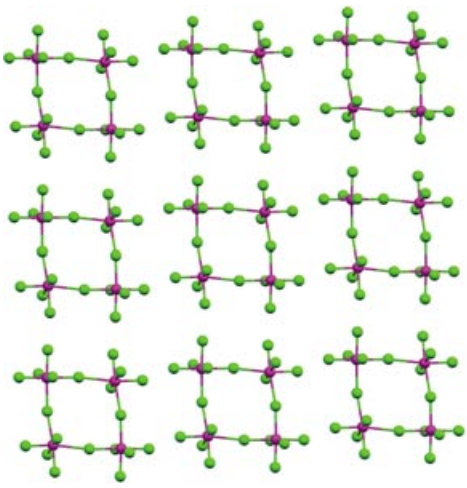

Figure 12. Packing of the $[(SbCl_5)_4]^{8-}$ tetrameric anions present in the *ab* plane of the crystal structure of $[1,4'\text{-Hbipy}][SbCl_5]$ (**8**). The analogous packing in $[2,2'\text{-H}_2\text{bipy}][SbCl_5]$ (**7**) is essentially identical.

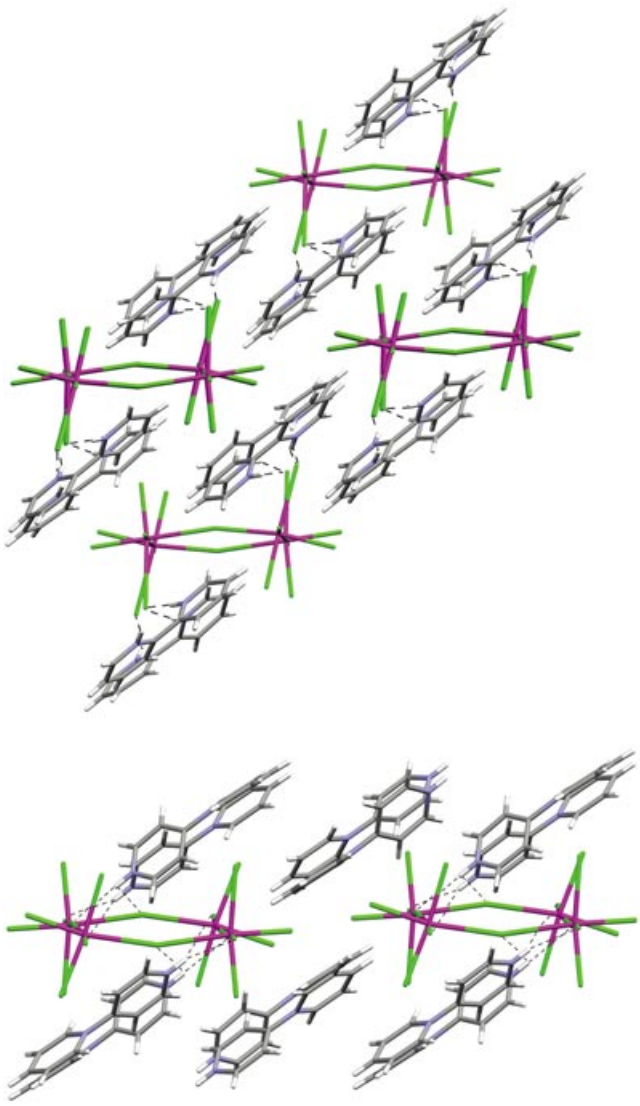

Figure 13. Top: Packing of $[(SbCl_5)_4]^{8-}$ and bipyridinium units present in the crystal structure of $[2,2'\text{-H}_2\text{bipy}][SbCl_5]$ (**7**) viewed parallel to the *ab* plane of the unit cell showing the N–H···Cl hydrogen bonds. Bottom: Packing of $[(SbCl_5)_4]^{8-}$ and bipyridinium units present in the crystal structure of $[1,4'\text{-Hbipy}][SbCl_5]$ (**8**) viewed parallel to the *ab* plane of the unit cell. The N–H···Cl hydrogen bonds are indicated.

Discussion

The $[PtCl_4]^{2-}$ salt structures fall into two categories: 1) the $[4,4'\text{-H}_2\text{bipy}]^{2+}$ salt (**1**) and 2) those of $[2,2'\text{-H}_2\text{bipy}]^{2+}$, $[3,3'\text{-H}_2\text{bipy}]^{2+}$ and $[1,4'\text{-Hbipy}]^{2+}$. All show NH···Cl hydrogen bonds of normal dimensions.[19] Remarkably, despite the fact that these hydrogen bonds are in different locations in the structures of the last three salts (**2**, **3** and **4**), the basic crystal structure in these cases is the same, with all having the same space group (or nearly so, since **4** has no centre of inversion but otherwise the same symmetry as **2** and **3**), and very similar unit cell dimensions and packing of molecular tectons. While the local details of these structures do vary, it would seem that the formation of (classical) NH···Cl hydrogen bonds appropriate to the particular bipyridinium isomer present is possible without significantly disturbing the shape

fit of the tectons and the substantial electrostatic energy of interaction between the ions. Furthermore the synthon and molecular recognition behaviour in the key periodic motif of **4** is close to that in **1**. The unit cell volumes of **1**–**4** are notable for what they imply for packing efficiency in these isomeric species. The unit cell volume per formula unit (*V*/*Z* see Table 1) is 317.0 Å^3 for **1**, and 331.9, 329.7 and 329.2 Å^3 for **2**–**4** respectively (with standard uncertainties ca. 0.1 Å^3). Clearly the packing of planar ribbons in **1** is highly efficient in terms of filling space. This is presumably favourable in terms of the intermolecular enthalpy of packing and may compensate for less favourable intramolecular aspects of the structure, in particular the planar conformation of the dication (see reference [11] for evidence that biphenyl and related species are typically nonplanar in the gas phase).

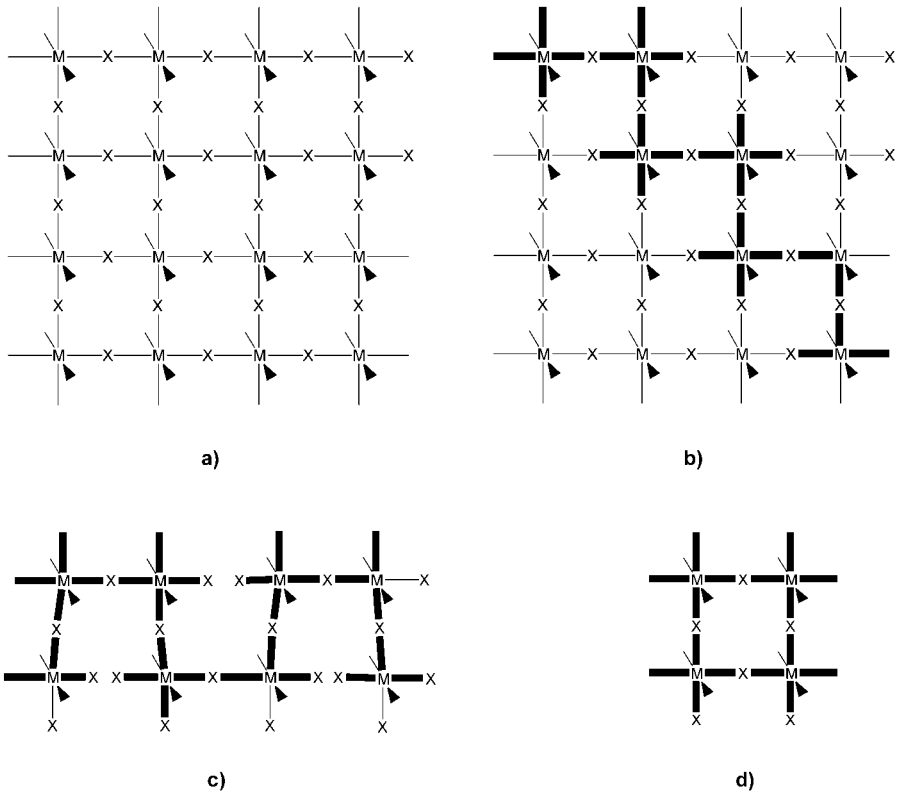

Figure 14. a) the MX_4 layer perovskite structure and various substructures (b–d) indicated in bold.

In the antimony system rather more flexibility is to be expected given the wide variety of oligomeric and polymeric structures known for the $[SbCl_5]^{2-}$ ion. Nevertheless the structures formed again fall in two camps: 1) the polymorphs of the $[4,4'\text{-}H_2bipy]^{2+}$ salt (**5a** and **5b**) and 2) the $[2,2'\text{-}H_2bipy]^{2+}$, $[3,3'\text{-}H_2bipy]^{2+}$ and $[1,4'\text{-}Hbipy]^{2+}$ salts (**6**, **7** and **8**). The structures of the **5a** and **5b** display chloride–bipyridinium hydrogen-bond motifs previously noted in our studies of the structures of salts of square planar and octahedral perchlorometallate anions. The set **6**–**8** are not strictly isostructural, but have the same space group, similar unit cells and very similar packing, differing principally in the mode of anion aggregation and the location of the NH···Cl hydrogen bonds. The layers of anions in these salts have structures that are formally related to the layer perovskite structures,[20] in which corner-sharing of MX_6 octahedra through bridging halides leads to a net of stoichiometry MX_4 (see Figure 14a). In the structure of **5b** a zig-zag substructure (Figure 14b) of the layer is preserved, while in **6** a battlement pattern (Figure 14c) of antimony chloride units is present and in **7** and **8** a single square (Figure 14d) is formally excised from the layer perovskite framework. While the gross crystal structures of **6**, **7** and **8** are broadly similar, the detail of the aggregation of the antimony chloride anions is apparently controlled by the cations, in particular by their hydrogen-bonding abilities. The unit cell volumes in this system are less informative than for **1**–**4**, because of the varied temperatures at which they were studied. Furthermore the cell volumes reflect the changes in the anion structures as well as the packing of the ions. The unit cell volumes per formula unit (*V*/*Z* see Table 3) for **5a**, **5b**, **6**, **7** and **8** are 389.7 (at ca. 293 K), 374.2 (at 173 K), 379.4 (at 173 K), 382.9 (at ca 293 K) and 377.3 Å^3 (at 173 K), respectively, with standard uncertainties of about 0.1 Å^3. Once again highest packing density is associated with the nearly planar ribbon motif, this time observed in **5b**. On this occasion the structure of highest packing efficiency is not the most stable, since **5b** transforms to **5a** readily.

In discussing the structures presented in this paper is important to recognise that we have not investigated exhaustively the possibility that the structures seen are but one of several polymorphs. This is of course possible (and in the case of **5** is known to occur). However, the mere fact of their observation (and that the bulk material apparently is composed of the only the form studied for all bar **5**) is indicative of the relative stability of the reported structures. Thus structures in which the primary supramolecular synthon is not apparently structure-directing are competitive and probably optimal. The observation of near isostructurality in salts of isomeric ions may also be interpreted as evidence of the possibility that (many) CH···Cl interactions can compensate for the loss or distortion of (a relatively small number of stronger) NH···Cl interactions (see reference [21] and references therein for a useful discussion of CH···Cl hydrogen bonding).

The message to draw from these observations is that while the primary (NH···Cl) hydrogen-bonding "supramolecular synthon" is important and does matter in determining

the local intermolecular geometry, the close-packing of the complex ions is also apparently important and the "best" structures result when these two factors complement one another. The successful design of molecular salts such as these will therefore require a careful balance of these various components of the lattice energy. The Desiraju–Wuest postulate—that molecular tectons with appropriate "sticky" supramolecular functionalities can be used to design and prepare crystal structures—is a useful, powerful and attractive insight. However, it is not complete and will necessarily require revision and development. In molecular salts, such as these studied here, it seems that electrostatic interactions *may* outweigh local hydrogen bonding effects and lead to crystal structures in which the molecular packing is apparently dominated by good shape fit and the Coulombic elements of the lattice energy.

The phenomenon of near-isostructural crystal forms of isomeric ions in halide salts is not confined to the examples shown in detail here. Jones[22] has reported an example in the salts of 2-chloromethylpyridinium chloride and 3-bromomethylpyridinium bromide as have Nättinen and Rissanen in the hydrochlorides of nicotinic acid chloride and isonicotinic acid chloride.[23] We have also observed similar behaviour in salts of tetrahedral $[MCl_4]^{2-}$ ions.[24]

In terms of the primary recognition motifs (or supramolecular synthons) by which the tectons in these systems interact, the information content in the NH···Cl motifs of the systems studied here is rather low, because of their relative simplicity. Much more complex, typically multipoint, interactions and neutral tectons are often used in synthetic crystallography.[1–4] It would seem likely that such information-rich means of molecular recognition are more likely to be robust synthons, especially for constructing solids composed of neutral tectons.

In the salts we and others have studied, we have placed emphasis on the network of NH···Cl and similar interactions and deliberately downplayed the significance of the numerous (usually longer) CH···Cl contacts that are present in all these structures. It is clear, and acknowledged that this simplification is not warranted, in the sense that the CH···Cl interactions must contribute significantly to the stability of the structures formed. However, the simplicity of this model is vital to its application in synthetic crystallography and crystal engineering. Unless we have models that qualitative and accessible to the chemist (as opposed to quantitative and only accessible through, say, substantial computational resources) there is little prospect of intuitive human input to the design of crystal structures.

Experimental Section

All pyridines, except 3,3′-bipyridine, were purchased from Lancaster or Aldrich and used without purification. 3,3′-Bipyridine was prepared according to the published procedure[25] and recrystallised as its hydrochloride salt from concentrated hydrochloric acid prior to use. Elemental analyses were performed by the School of Chemistry Microanalytical Service. Powder diffraction was carried out using a Bruker D8 diffractometer.

Synthesis of [3,3′-bipyridinium][$PtCl_4$] (2): A solution of 3,3-bipyridinium dichloride (0.106 g, 6.66×10^{-4} mol) in concentrated hydrochloric acid (5 mL) was added dropwise, with stirring, to a solution of potassium tetrachloroplatinate (0.277 g, 6.70×10^{-4} mol) in water (10 mL). The resulting orange suspension was stirred overnight, and then filtered. The solid obtained was washed with water (10 mL) and ethanol (10 mL), and then dried at the pump, (0.188 g, 3.80×10^{-4} mol, 57 %). Elemental analysis calcd (%): C 24.26, H 2.04, N 5.66; found: C 24.20, H 1.95, N 5.50. Single crystals were grown by dissolution of the product in hot aqueous hydrochloric acid followed by slow cooling.

Synthesis of [2,2′-bipyridinium][BF_4]$_2$: Tetrafluoroboric acid (2.2 mL, 54 %wt solution in diethyl ether, 1.18 g, 13.44×10^{-3} mol) was added dropwise, with stirring, to a solution of 2,2′-bipyridine (1.06 g, 6.79×10^{-3} mol) in acetonitrile (30 mL). The resulting suspension was stirred overnight. Diethyl ether (150 mL) was added and the suspension filtered. The solid obtained was washed with diethyl ether (20 mL) and dried at the pump (2.16 g, 6.51×10^{-3} mol, 95.9 %). Elemental analysis calcd (%):C 36.20, H 3.05, N 8.44; found: C 36.05, H 2.95, N 8.07.

Synthesis of [$PhCH_2PPh_3$][$PtCl_4$]: Benzyltriphenylphosphonium chloride (1.05 g, 2.70×10^{-3} mol) was added To a solution of potassium tetrachloroplatinate (0.56 g, 1.33×10^{-3} mol) in distilled water (50 mL). Dichloromethane (100 mL) was added and the resulting mixture stirred overnight. The dichloromethane layer was separated and the water layer extracted with dichloromethane (3×50 mL). The dichloromethane fractions were combined and dried over magnesium sulfate. The solvent was removed under reduced pressure leaving the product as a dark orange powder (1.28 g, 1.23×10^{-3} mol, 92.2 %). Elemental analysis calcd (%): C 57.49, H 4.25; found: C 56.60, H 3.73.

Synthesis of [2,2′-bypyridinium][$PtCl_4$] (3): A solution of 2,2′-bipyridinium bis tetrafluoroborate (0.088 g, 2.65×10^{-4} mol) in acetonitrile (5 mL) was added dropwise, with stirring, to a solution of bis(benzyltriphenylphosphonium) tetrachloroplatinate (0.263 g, 2.52×10^{-4} mol) in acetonitrile (10 mL). Immediately upon addition a yellow precipitate was observed. The suspension was stirred for five minutes, until precipitation was complete. The suspension was filtered and washed with acetonitrile (10 mL) and diethyl ether (10 mL), and then dried at the pump (0.083 g, 1.68×10^{-4} mol, 66.7 %). Elemental analysis calcd (%): C 24.26, H 2.04, N 5.66; found: C 24.43, H 1.55, N 5.24 Single crystals were grown by mixing stoichiometric amounts of K_2PtCl_4 and 2,2′-bipyridine in aqueous hydrochloric acid followed by slow evaporation.

Synthesis of [1-(4′-pyridinium)pyridinium][$PtCl_4$] (4): A solution of pyridylpyridinium chloride hydrochloride (0.103 g, 4.50×10^{-4} mol) in water (5 mL) and concentrated HCl (10 mL) was added dropwise, with stirring, to a solution of K_2PtCl_4 (0.186 g, 4.48×10^{-4} mol) in water (10 mL). The resulting orange solution was reduced in volume (5 mL) and allowed to cool to room temperature. Upon cooling orange crystals grew, which were filtered off, washed with ice cold water (2 mL) and ethanol (2 mL), and then dried at the pump (0.165 g, 3.33×10^{-4} mol, 74.4 %). Elemental analysis calcd (%): C 24.26, H 2.04, N 5.66; found: C 24.04, H 1.95, N 5.40.

Synthesis of [4,4′-bipyridinium][$SbCl_5$] (5b): A solution of 4,4′-bipyridine (0.350 g, 2.21×10^{-3} mol) in concentrated hydrochloric acid (10 mL) was added dropwise, with stirring, to a solution of antimony trichloride (0.507 g 2.22×10^{-3} mol) in concentrated hydrochloric acid (10 mL). The resulting yellow solution was heated to reduce the volume (15 mL), then allowed to cool to room temperature. The product crystallized as an intimate mixture of red plates and yellow needles. The red plates revert to yellow after a few hours. Immediately after crystallization, a suitable red plate was selected and mounted on the diffractometer under a stream of cold nitrogen . The remaining crystals were allowed to cool, were filtered off and washed with cold concentrated hydrochloric acid (5 mL) and cold ethanol (5 mL), and then dried at the pump (0.565 g, 1.24×10^{-3} mol, 56 %).

Synthesis of [3,3′-bipyridinium][$SbCl_5$] (6): A solution of 3,3′-bipyridinium dichloride (0.308 g, 1.34×10^{-3} mol) in concentrated hydrochloric acid (10 mL) was added dropwise, with stirring, to a solution of antimony trichloride (0.306 g 1.34×10^{-3} mol) in concentrated hydrochloric acid (10 mL). The resulting colorless suspension was heated to redissolve and reduce the volume (15 mL). The solution was allowed to cool to room temperature and left to crystallize. The colorless crystals were filtered,

washed with ice cold water (2 mL) and ethanol (5 mL), and then dried at the pump, (0.350 g, 7.65×10^{-4} mol, 57%). Elemental analysis calcd (%): C 26.27, H 2.20, N 6.13; found: C 26.09, H 1.97, N 5.95.

Synthesis of [4-pyridylpyridinium][$SbCl_5$] (8): Antimony trichloride (0.228 g, 1.00×10^{-3} mol) was added dropwise, with stirring, to a solution of 4-pyridylpyridinium chloride hydrochloride (0.229, 1.00×10^{-3} mol) in water (5 mL) and concentrated hydrochloric acid (5 mL). The resultant green/yellow solution was heated to reduce the volume (5 mL) and after slow cooling, clear yellow crystals were formed. The crystals were filtered, were washed with ice cold water (2 mL) and ethanol (5 mL), and then dried at the pump, (0.198 g, 4.33×10^{-4} mol, 43.3%). Elemental analysis calcd (%): C 26.24, H 2.19, N 6.12; found: C 26.36, H 2.22, N 5.98. Crystals suitable for X-ray diffraction were prepared by evaporation of a solution of the product in dilute aqueous hydrochloric acid on a watch-glass.

General X-ray crystal structure information: Diffraction measurements, **2**, **3**, **4**, **5b**, **6** and **8**, were made at −100°C on a Bruker-AXS SMART three-circle CCD diffractometer using graphite monochromated $Mo_{K\alpha}$ radiation ($\lambda=0.71073$ Å).[26] Unit cell dimensions were determined from reflections taken from three sets of ten frames (at 0.3° steps in ω), each at 10 s exposure. Data frames were referenced to a set of ten dark frame readings each taken at n s exposures without X-rays, whereby n s is the time for each exposure during data collection. For crystals of monoclinic or higher crystal symmetry, a hemisphere of reciprocal space was scanned by 0.3 ωsteps at ϕ 0, 88 and 180° with the area detector center held at $2\theta=-27°$. For triclinic crystals, a full sphere of reciprocal space was scanned. In all experiments, each exposure was n s (typically, $10\le n\le40$). The reflections were integrated using the SAINT program.[26] Absorption, Lorentz and polarization corrections were applied. The structures were solved by direct methods and refined using full-matrix least-squares against F^2 using SHELXTL.[26] All non-hydrogen atoms were assigned anisotropic displacement parameters and refined without positional constraints. Hydrogen atoms were included in idealized positions with isotropic displacement parameters constrained to 1.5 times the U_{eq} of their attached carbon atoms for methyl hydrogens, and 1.2 times the U_{eq} of their attached carbon. Many of the details of the structure analyses of **2**, **3**, **4**, **5b**, **6**, **7**, and **8** are presented in Table 2.

CCDC-231530–231535 contain the supplementary crystallographic data for this paper. These data can be obtained free of charge via www.ccdc.cam.ac.uk/conts/retrieving.html (or from the Cambridge Crystallographic Data Centre, 12 Union Road, Cambridge CB21EZ, UK; fax: (+44) 1223-336-033; or deposit@ccdc.cam.uk).

X-ray powder diffraction experiments on bulk samples of **2**, **3**, **4**, **5b**, **6**, **7** and **8** were consistent with the presence of pure phases with the structure identified by single crystal methods.

Acknowledgements

We thank the EPSRC and the University of Bristol for financial support.

[1] a) M. Simard, D. Su, J. D. Wuest, *J. Am. Chem. Soc.* **1991**, *113*, 4696; b) J. H. Fournier, T. Maris, J. D. Wuest, W. Z. Guo, E. Galoppini, *J. Am. Chem. Soc.* **2003**, *125*, 1002.
[2] S. Mann, *Nature* **1993**, *365*, 499.
[3] A. Jouaiti, M. W. Hosseini, N. Kyritsakas, *Chem. Commun.* **2003**, 472, and references therein.
[4] a) G. R. Desiraju, *Angew. Chem.* **1995**, *107*, 2541; *Angew Chem. Int. Ed. Engl.* **1995**, *34*, 2311; b) G. R. Desiraju, *Chem. Commun.* **1997**, 1475.
[5] a) G. R. Lewis, A. G. Orpen, *Chem. Commun.* **1998**, 1873; b) A. L. Gillon, A. G. Orpen, J. Starbuck, X.-M. Wang, Y. Rodríguez-Martín, C. Ruiz-Pérez, *Chem. Commun.* **1999**, 2287; c) A. L. Gillon, G. R. Lewis, A. G. Orpen, S. Rotter, J. Starbuck, X.-M. Wang, Y. Rodriguez-Martin, C. Ruiz-Pérez, *J. Chem. Soc. Dalton Trans.* **2000**, 3897.
[6] B. Dolling, A. L. Gillon, A. G. Orpen, J. Starbuck, X.-M. Wang, *Chem. Commun.* **2001**, 567.
[7] a) A. Angeloni, A. G. Orpen, *Chem. Commun.* **2001**, 343; b) T. J. Podesta, A. G. Orpen, *CrystEngComm* **2002**, *4*, 336.
[8] a) J. C. M. Rivas, L. Brammer, *Inorg. Chem.* **1998**, *37*, 4756; b) L. Brammer, J. K. Swearingen, E. A. Bruton, P. Sherwood, *Proc. Natl. Acad. Sci. USA* **2002**, *99*, 4956.
[9] S. Ferlay, V. Bulach, O. Felix, M. W. Hosseini, J. M. Planeix, N. Kyritsakas, *CrystEngComm* **2002**, 447.
[10] a) D. Braga, L. Maini, M. Polito, E. Tagliavini, F. Grepioni, *Coord. Chem. Rev.* **2003**, *246*, 53; b) K. T. Holman, A. M. Pivovar, J. A. Swift, M. D. Ward, *Acc. Chem. Res.* **2001**, *34*, 107; c) C. B. Aakeroy, K. Beffert, J. Desper, E. Elisabeth, *Cryst. Growth Des.* **2003**, *34*, 837; d) V. Bertolasi, L. Pretto, P. Gilli, V. Ferretti, G. Gilli, *New J. Chem.* **2002**, *26*, 1559.
[11] C. P. Brock, R. P. J. Minton, *J. Am. Chem. Soc.* **1989**, *111*, 4586.
[12] A. G. Orpen, M. J. Quayle, *J. Chem. Soc. Dalton Trans.* **2001**, 1601.
[13] a) A. Z. Lipka, *Z. Anorg. Allg. Chem.* **1980**, *469*, 218; b) A. Ohta, Y. Yamashita, *Mol. Cryst. Liq. Cryst. Sci. Technol. Sect. A* **1997**, *296*, 1; c) F. Cariati, A. Panzanelli, L. Antolini, L. Menabue, G. C. Pellacani, G. Marcotrigiano, *J. Chem. Soc. Dalton Trans.* **1981**, 909; d) J. Zaleski, A. Pietraszko, *J. Mol. Struct.* **1994**, *327*, 287; e) K. Matsumoto, S. Z. Ooi, *Kristallogr. Kristallgeom. Kristallphys. Kristallchem.* **1979**, *150*, 139; f) M. B. Hursthouse, K. M. A. Malik, P. K. Bakshi, A. A. Bhuiyan, M. Q. Ehsan, S. Z. Haider, *J. Chem. Crystallogr.* **1996**, *26*, 739; g) M. Bujak, J. Zaleski, *Acta Crystallogr. Sect. C* **1999**, *55*, 1775; h) M. Bujak, J. Zaleski, *Z. Naturforsch. Teil B* **2001**, *56*, 521.
[14] J. Valdés-Martínez, M. Del Rio-Ramirez, S. Hernández-Ortega, C. B. Aakeröy, B. Helfrich, *Cryst. Growth Des.* **2001**, *1*, 485.
[15] A. Lipka, *Z. Anorg. Allg. Chem.* **1980**, *469*, 229.
[16] A. Lipka, *Z. Naturforsch. Teil B* **1983**, *38*, 1615.
[17] a) N. W. Alcock, *Adv. Inorg. Chem. Radiochem.* **1972**, *15*, 1; b) N. W. Alcock, *Bonding and Structure*, Ellis Horwood, Chichester, **1990**.
[18] J. Starbuck, N. C. Norman, A. G. Orpen, *New J. Chem.* **1999**, *23*, 969.
[19] G. Aullón, D. Bellamy, L. Brammer, E. A. Bruton, A. G. Orpen, *Chem. Commun.* **1998**, 653; L. Brammer, E. A. Bruton, P. Sherwood, *Cryst. Growth Des.* **2001**, *1*, 277.
[20] a) D. B. Mitzi, *Prog. Inorg. Chem.* **1999**, *48*, 1; b) P. Day, *J. Chem. Soc. Dalton Trans.* **1997**, 701; c) G. S. Long, M. Y. Wei, R. D. Willett, *Inorg. Chem.* **1997**, *36*, 3102.
[21] J. Hassan, V. Penalva, L. Lavenot, C. Gozzi, M. Lemaire, *Tetrahedron* **1998**, *54*, 13793.
[22] J. A. van den Berg, K. R. Seddon, *Cryst. Growth Des.* **2003**, *3*, 643.
[23] P. G. Jones, *CrystEngComm* **2003**, *5*, 303.
[24] K. I. Nättinen, K. Rissanen, *CrystEngComm* **2003**, *5*, 326.
[25] P. Crawford, A. G. Orpen, T. J. Podesta, B. Salt, unpublished results.
[26] SMART, Copyright 1989–1999, Bruker AXS, Madison, WI (USA); SAINT, Bruker AXS, Madison, WI (USA); SHELXTL, Rev. 5.0, Bruker AXS, Madison, WI (USA).

Received: February 18, 2004
Published online: June 15, 2004

